Lime muds and their genesis off-Northwestern India during the late Quaternary

V Purnachandra Rao[1,*], A Anil Kumar[1,4], S W A Naqvi[1], Allan R Chivas[2], B Sekar[3] and Pratima M Kessarkar[1]

[1]*National Institute of Oceanography, Dona Paula 403 004, Goa, India.*
[2]*Geo-QUEST Research Centre, School of Earth and Environmental Sciences, University of Wollongong, NSW 2522, Australia.*
[3]*Birbal Sahni Institute of Paleobotany, Lucknow 226 007, India.*
[4]*Present address: Marine and Coastal Survey Division, Geological Survey of India, Pandeshwar, Mangalore, Karnataka.*
[*]*Corresponding author. e-mail: vprao@nio.org*

Two sediment types were found in five gravity cores collected from water depths between 56 m and 121 m along the northwestern continental margin of India: lime muds were abundant in the lower section while siliciclastic sediments dominated the upper section. Lime mud-dominated sediments in shelf cores contained 60%–75% carbonate, 0.3%–0.6% Sr and terrigenous minerals, whereas those at the shelf break were found to have >90% carbonate, 0.6%–0.8% Sr and traces of terrigenous minerals. Aragonite needles showing blunt edges, jointed needles and needles wrapped in smooth aragonite cement were found to be common. Stable (O and C) isotopes of lime mud indicate a potentially freshwater contribution for shelf cores and purely marine contribution for those at the shelf break. Calibrated radiocarbon ages of the lime muds ranged from 17.6–11.9 ka in different cores. The results reported here suggest that the lime muds in the shallow shelf are probably reworked from the Gulf of Kachchh, whereas those at the shelf break were biodetrital, initially formed on the carbonate platform during low stands of sea level and then exported. The change in lime mud-dominated to siliciclastic-dominated sediments in the cores may be due to climate change and rapid rise in sea level during the early Holocene.

1. Introduction

Lime muds are produced by several mechanisms: mechanical disintegration of biogenic skeletal components, disaggregation of calcareous green algae, inorganic precipitation, bioerosion, erosion of tidal-flat deposits and bio-geochemical processes (Bathurst 1971). The modern settings for lime mud formation are largely confined to carbonate platforms (Bahamas, Florida and Belize) or shallow-water ramps (Persian Gulf) (Ginsburg 1956; Lowenstam and Epstein 1957; Cloud 1962; Wells and Illing 1964; De Groot 1965; Matthews 1966; Stockman *et al* 1967; Mitterer 1972; Neumann and Land 1975; Steinen *et al* 1988; Boardman and Carney 1991; Robbins and Blackwelder 1992; Milliman *et al* 1993; Gischler and Lomando 1999; Dix 2001; Gischler and Zingeler 2002; Roth and Reijmer 2004, 2005). Lime muds constitute ∼30–50% of the Holocene sediments in the *Halimeda* bioherms from the Great Barrier Reef (Marshall and Davies 1988). Modern calcareous tube-pelagic muds, spiculitic and bryozoan silts and late Quaternary carbonate muds

Keywords. Lime muds; late Quaternary; sea level; radiocarbon ages; stable isotopes; western India.

J. Earth Syst. Sci. **121**, No. 3, June 2012, pp. 769–779

are reported on the northwestern and southwest Australian margins (James *et al* 1999, 2001, 2004, 2005; Dix *et al* 2005). Fine-grained carbonates are also common in reef environments (Adjas *et al* 1990).

Several researchers have attempted to explain the formation of lime mud in modern carbonate settings. Inorganic formation is favoured by Cloud (1962); Wells and Illing (1964); De Groot (1965); Milliman *et al* (1993); Dix (2001) and Dix *et al* (2005), whereas disintegration of codiacean algae and other skeletal materials is favoured by Lowenstam and Epstein (1957); Matthews (1966); Stockman *et al* (1967); Neumann and Land (1975) and James *et al* (1999, 2001, 2004). Lime mud origin has been linked to dense carbonate mud suspensions (whitings) formed from precipitation of fine-grained aragonite in the water column (Broecker and Takahashi 1966; Morse *et al* 1984; Morse and Mackenzie 1990; Robbins and Blackwelder 1992). Shinn *et al* (1989) have also reported that the whitings have resulted from the resuspension of deposited lime mud because of stirring by fish/ocean currents/storms. Lime mud formation through micritization, diminution (Reid *et al* 1992) and syndepositional recrystallization of sediment grains (Miliolid foraminifera and *Halimeda*) (Macintyre and Reid 1995; Reid and Macintyre 1998) has also been reported. Yates and Robbins (1999) proposed radioisotope tracer of inorganic carbon and Ca for identifying microbial carbonate precipitates. The Sr-rich aragonites of the eastern Mediterranean sapropels have been proposed to be of diagenetic origin (Thomson *et al* 2004) or from detrital/biogenic source, disintegrated from *Halimeda* (Reitz and de Lange 2006). This paper investigates the origin of lime muds from the open-ocean shelf off northwest India and the influence of climate and sea level changes on their deposition.

1.1 *Geological setting*

A drowned carbonate platform is the largest topographic feature on the northwestern continental margin of India (figure 1). This platform was isolated from the coast by a huge clastic depocentre – the Dahanu depression, in which pro-delta sediments have been deposited since the Eocene (Basu *et al* 1980). This depression is now filled and forms the inner shelf, consisting of modern siliciclastic sediments. The eastern margin of the platform is now connected to the inner shelf and the platform thus forms an outer shelf of relic sandy carbonate sediments with water depths ranging between 60 and 110 m. As the western slopes of the platform are steep, the term 'carbonate ramp' does not apply. Accordingly, we prefer to use the term

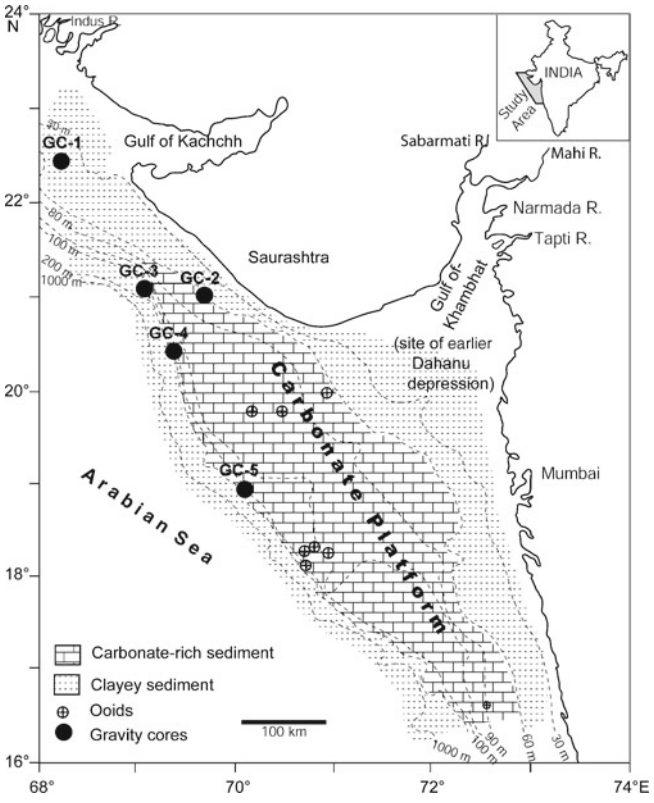

Figure 1. Location of the gravity cores along the northwestern continental margin of India.

'drowned platform'. The relic deposits on the platform consist of abundant aragonite faecal pellets, ooids, *Halimeda* grains and a few bivalves, benthic and planktic foraminifers (Rao and Wagle 1997; Rao *et al* 1994). Also present are indurated aragonite muds, *Halimeda*- and pelletal limestones, coralline algal nodules, minor coral fragments, oyster shells and dolomite encrustations (Nair 1971; Nair *et al* 1979; Rao *et al* 1994, 2003). The radiocarbon ages of the above largely range between 12,940 ^{14}C yr BP (14.3 cal. ka) and 7,250 ^{14}C yr BP (7.6 cal. ka) (Rao *et al* 2003). Vaz *et al* (1993) reported lime muds between 150 and 500 m water depth off the Gulf of Kachchh and suggested that these lime muds are detrital and transported from shallow depths.

2. Materials and methods

Five gravity cores, two from the continental shelf (GC-1, GC-2) and three from the shelf break (GC-3 to GC-5) between 56 and 121 m water depth (figure 1), collected during the 148th cruise of *ORV Sagar Kanya,* were studied. Core lengths ranged from 5 to 7 m. The cores were sectioned onboard at 2 cm intervals in the upper 2 m but at 5 cm intervals thereafter.

Table 1. *Details of radiocarbon analyses on different sediment sections of the cores.*

Sl. no.	Core no., length (m) of the sediment recovered	Water depth (m)	Depth interval dated (cm)	BSIP no.	Measured age (yr BP)	Corrected age (yr BP)	Calibrated age (ka BP)
1	GC-1/SK-148/22; 7.02	56	70–74	2020	8990 ± 100	8427	9.38
2	;;		105–110	2000	12670 ± 200	12107	14.05
3	;;		140–145	2019	12230 ± 140	11667	13.54
4	;;		200–205	1804	11330 ± 140	10767	12.76
5	;;		305–310	2001	13250 ± 120	12687	14.52
6	;;		400–405	1780	15370 ± 550	14807	17.60
7	GC-2/SK-148/31; 5.98	65	20–22	1891	7810 ± 100	7247	8.07
8	;;		60–62	1792	9950 ± 290	94387	10.55
9	;;		74–82	2004	11130 ± 140	10567	12.46
10	;;		148–150	2032	10910 ± 220	10347	12.00
11	;;		220–235	2030	11610 ± 280	11047	12.98
12	;;		560–565	2017	11340 ± 160	10777	12.78
13	GC-3/SK-148/30, 5.49	121	26–30	1985	5220 ± 100	4657	5.41
14	;;		98–102	1963	10230 ± 100	9667	10.74
15	;;		124–126	2024	12980 ± 250	12417	14.52
16	;;		136–138	1973	12700 ± 140	12137	13.99
17	;;		360–365	1980	14070 ± 130	13507	16.10
18	GC-4/SK-148/32, 4.37	111	26–28	1959	6380 ± 70	5817	6.64
19	;;		96–100	1979	8240 ± 120	7677	8.53
20	;;		178–180	2028	10840 ± 160	10277	11.91
21	;;		210–215	1984	11430 ± 150	1030	12.81
22	;;		370–375	1975	11060 ± 200	10497	12.29
23	GC-5/SK-148/43 2.83	115	26–28	2015	11780 ± 120	11217	13.05
24	;;		95–100	2034	12800 ± 180	12237	14.09
25	;;		210–215	2035	12720 ± 120	12157	13.99
26	;;		270–275	2022	12760 ± 180	12197	14.08

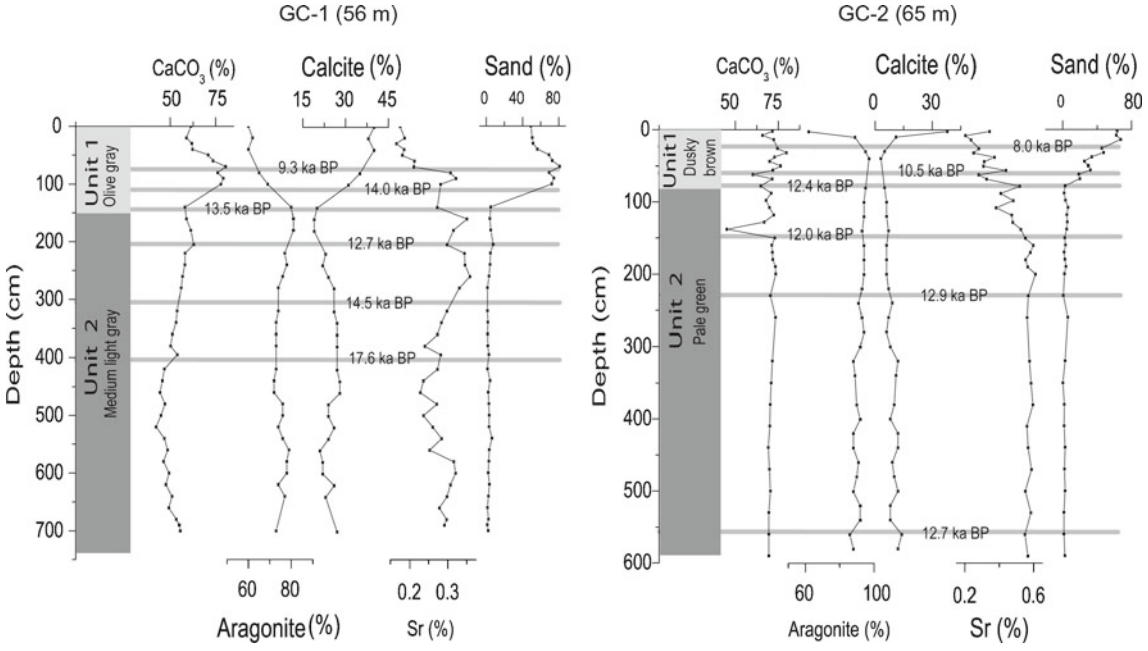

Figure 2. Distribution of carbonate, calcite and aragonite content, Sr content and sand content in the shelf cores: GC-1 and GC-2.

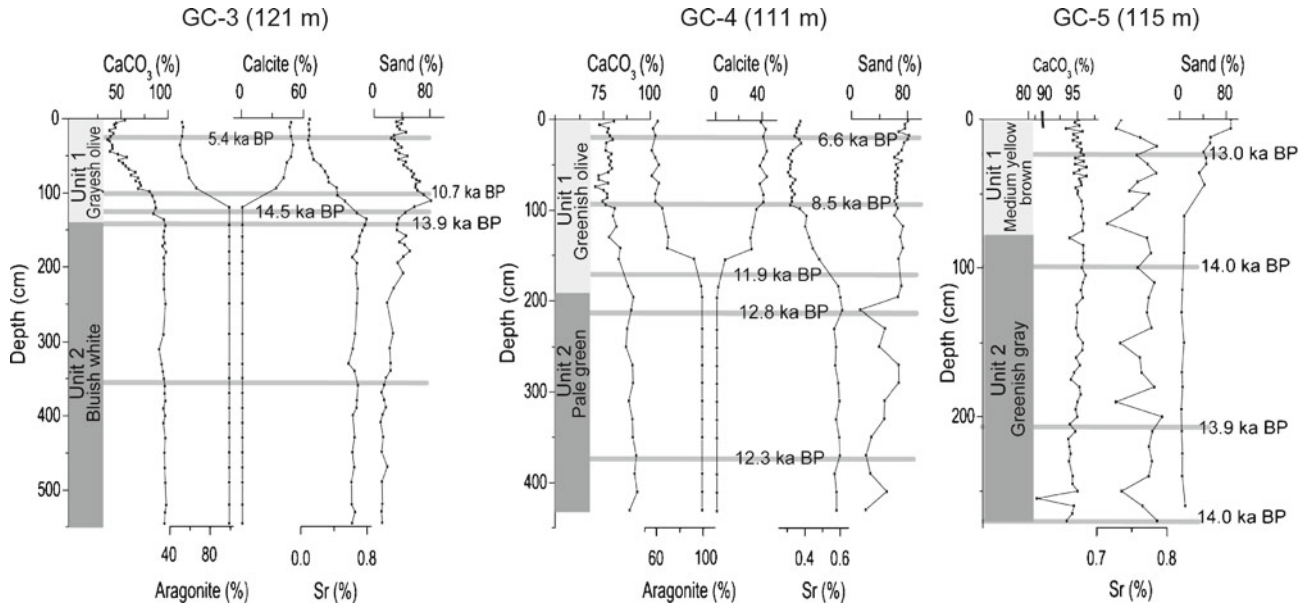

Figure 3. Distribution of carbonate, calcite and aragonite content, Sr content and sand content in the cores GC-3, GC-4 and GC-5 at the shelf break.

Samples from each core (35–66 samples) were selected and calcium carbonate content in a total of 230 sediment samples was measured by weight loss following acidification with 0.1N HCl. Every fifth sample was replicated and reproducibility found to be <5%. Mineralogy was determined by scanning from 25° 2θ to 35° 2θ at 1° 2θ/min on a Philips X-ray diffractometer using nickel-filtered Cu K α radiation. Peak heights of carbonate mineral reflections are measured above the background and weight percentages of minerals were determined using the calibration curve prepared based on mixtures of pure aragonite and calcite. The <63 μm fraction of the sediment was separated by wet sieving following removal of soluble salts by water washing and organic matter by H_2O_2 and examined under a JEOL 5800 LV scanning electron microscope (SEM). The 63–125 μm fraction of the sediment was also examined.

Bulk sample powders of 0.1 to 0.2 g were weighed and dissolved in 1N HCl for 1 hr at room temperature. The acid-insoluble residue was separated through filtration. The total volume of the filtrate was made up to 100 ml. These solutions together with the standards were analysed for Sr content by using ICP-AES and the weight percentage of Sr relative to total sediment was reported. The accuracy and reproducibility of the results were found to be <5%. Lime muds with more than 70–80 wt% aragonite were analyzed for stable isotopes. The mud fraction of the samples from two cores was treated with 5.3% aqueous solution of sodium hypochlorite for 24 hr to remove the organic matter and was subsequently washed and dried for oxygen and carbon isotope analysis at the University of Wollongong, using Micromass PRISM III mass spectrometer with a Multiprep acid-on-individual-carbonate device with analytical conditions (Chivas *et al* 2002). The precisions of the results for δ^{13}C and δ^{18}O were found to vary from 0.02‰ to 0.07‰ and 0.04‰ to 0.12‰, respectively. Bulk samples of lime mud from each core were sent to Birbal Sahni Institute of Palaeobotany (BSIP), Lucknow, for radiocarbon age measurements. Measured ^{14}C ages were calibrated using CALIB rev. 4.3 of Stuiver *et al* (1998). During calibration, a local deviation in $\Delta R - 163 \pm 30$ for the northern Arabian Sea was used (Dutta *et al* 2001). Calibrated ages (referred here as ka) are discussed in the text (table 1). Core logs showing colour, carbonate and sand content, Sr content and radiocarbon ages are depicted in figures 2 and 3. The SEM photos of lime muds are given in figure 4 and scatter plot using stable isotopes of lime muds in figure 5.

3. Results

The sediments in the gravity cores exhibited two distinct sedimentary units, a lower unit 2 and an upper unit 1. Unit 2 consisted of abundant lime muds, whereas unit 1 consisted of a mixture of terrigenous and carbonate sediments, or predominantly terrigenous sediments.

3.1 *Gravity cores from the continental shelf (GC-1 and GC-2)*

Lime muds predominated in unit 2 of these cores and that contained 50–60% carbonate in GC-1 and

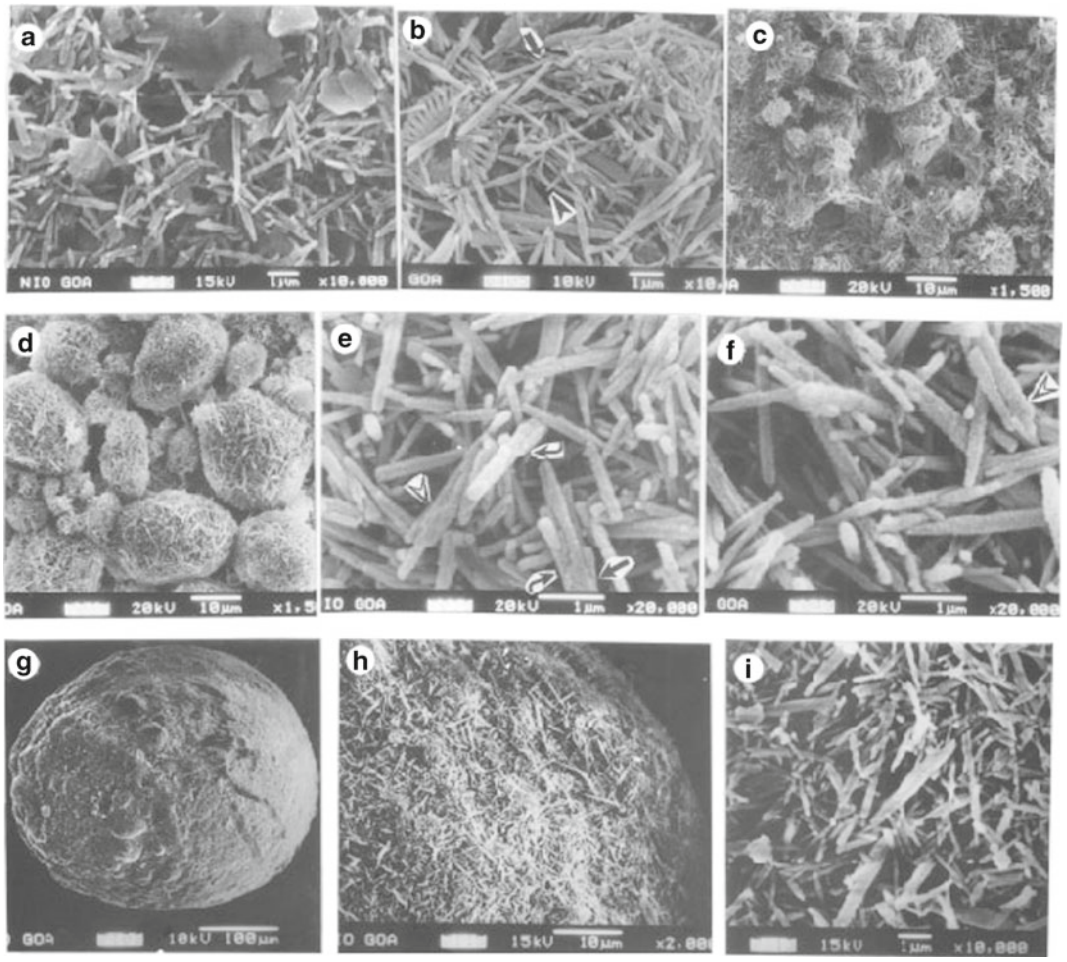

Figure 4. Scanning Electron Micrographs (SEM) of lime muds: (**a**) Aragonite needles associated with detrital particles in core GC-1; (**b–f**) SEM photographs of lime muds occurring in cores at the shelf break; (**b–c**) aragonite needles showing blunting at the edges; (**d**) spheroid to ovoid type aragonite particles; (**e–f**) needles showing jointed needles and needles enveloped in a smooth aragonite (between arrows in 'e'); (**g–i**) SEM photographs of lime muds in the coarse fractions; (**g**) Aragonite spheres in 125–250 μm fraction showing that the larger sphere is an aggregate of small spheres; (**h**) high-magnification of 'g' at the edges, and (**i**) further magnification of 'h' showing blunt aragonite needle edges.

∼75% in GC-2 (figure 2). The aragonite content of carbonates varied from 73% to 80% in GC-1, but was higher than 90% in GC-2. Aragonite needles exhibited blunt edges and were associated with detrital particles (figure 4a). Sand content in unit 2 of the cores was <5%. In GC-1 it comprised mica, quartz, pyrite, rounded bioclasts/pellets, *Uvigerina sp.* and ostracods at different intervals. In GC-2, it comprised subrounded-to-rounded bioclasts, pelletal material, and a few ostracods and bivalves at different intervals. The unit 1 sediments of GC-1 core comprised green grains, green clay infillings of planktic/benthic foraminifers and their aggregates.

The average Sr content of the lime muds (unit 2) was 0.29% in GC-1 and 0.55% in GC-2. Sr content increases with increasing weight percentage of aragonite in GC-2 (figure 5a). It gradually decreased from transition to the core top of unit 1 sediments in both cores. The δ^{18}O values of the lime muds ranged between −0.1‰ and −0.5‰ and, −0.3‰ and −0.5‰ in GC-1 and GC-2, respectively. Similarly, the δ^{13}C values ranged between 2.6‰ and 2.9‰ and, 2.4‰ and 3.0‰ in GC-1 and GC-2, respectively (table 2). The isotope values of lime muds formed a separate group (figure 5b, c).

The age of lime muds of GC-1 and GC-2 ranged between 17.6 and 12.8 ka and 13.0 and 12.0 ka, respectively (table 1). Older sediments overlay the younger sediments in unit 2 sediments of both the cores (figure 2).

3.2 *Gravity cores from the shelf break (GC-3, GC-4, GC-5)*

The lime muds (unit 2) contained 90–95% carbonate in GC-3–GC-5 (figure 3). The weight percent of aragonite was >95 and low-Mg calcite was <5.

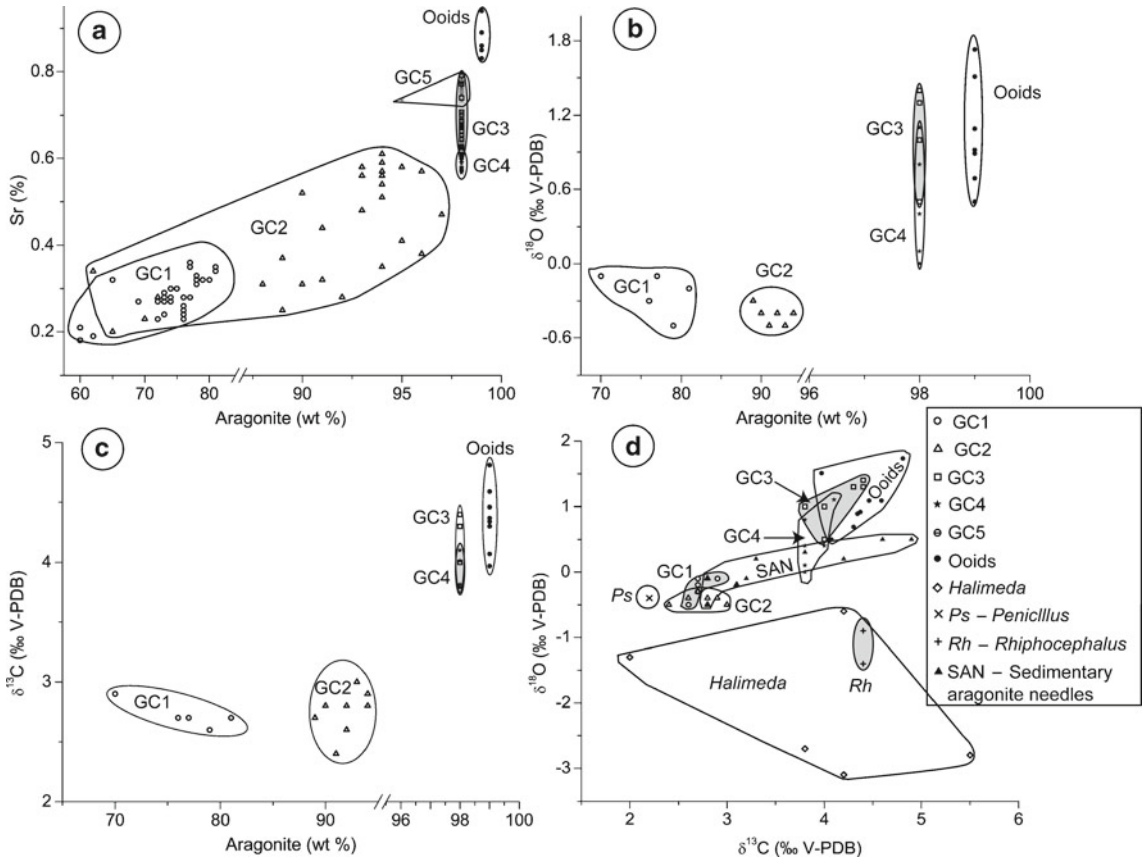

Figure 5. Scatter plots of the lime muds. Weight percentage of aragonite *versus* Sr (**a**), δ^{18}O (**b**), δ^{13}C (**c**). (**d**) A plot between δ^{13}C and δ^{18}O. Stable isotope values of *Halimeda, Penicillus, Riphocephalus* and sedimentary aragonite needles (see table 2) are from Lowenstam and Epstein (1957). Ooid data (unpublished data of Rao and Milliman).

The sand content of unit 2 sediments in GC-3 and GC-4 was relatively higher (25–50%) than in GC-5 (<25%). The sand comprised largely spherical to ovoid particles and pelletal material, which were aragonitic in composition. The unit 1 sediments of GC-3 and GC-4 were more terrigenous in nature, which increased with decrease in carbonate content (figure 3).

Lime muds under SEM exhibited clusters or aggregates morphologically similar to spheroid or ovoid-type particles (figure 4b–d). Repeated investigations on the untreated and H_2O_2-treated lime muds confirmed the presence of spheroids and ovoid-type particles. On higher magnification, the spheroid or ovoid-type particles consisted of wrapped aragonite needles. The needles exhibited rounded ends or blunt edges. Jointed partly radiating needles (figure 4e–f) and needles wrapped in a smooth envelope of aragonite (see between arrows in figure 4e) were also seen. In some cases coccoliths were associated with the aragonite needles (figure 4b). Lime muds in the size fractions 63–125 μm and >125 μm also contained similar spherical and ovoid particles, formed by aggregation of aragonite needles. Figure 4(g) shows larger sphere composed of aggregates of smaller spheres. These spheres also contained wrapped aragonite needles (figure 4h–i). In fact, abundance of these particles increased the sand content in unit 2 sediments of GC-3 and GC-4 (figure 3). Heavily fragmented prismatic or smaller rods of aragonite needles were also seen at some places.

The average Sr content of the lime muds was 0.66% in GC-3, 0.58% in GC-4 and 0.77% in GC-5. Plot of Sr *vs.* aragonite content showed that Sr values of ooids were the highest, lime muds of GC-4 were lowest and Sr of lime muds of GC-3 and GC-5 plot below ooids and above lime muds of GC-4. The Sr values in unit 1 sediments of GC-3 and GC-4 decreased from transition to the core top but remained high (avg. 0.76%) in GC-5.

The δ^{18}O and δ^{13}C values of lime mud ranged between 0.0‰ and 1.4‰ and between 3.8‰ and 4.4‰, respectively (table 2). The isotopic values of lime muds were within, or slightly lower than the range for ooids (see figure 5b–c), but within the range of values for sedimentary aragonite needles (see figure 5d). The radiocarbon ages of the lime

Table 2. *Distribution of aragonite, stable isotope ratios of carbon ($\delta^{13}C$) and oxygen ($\delta^{18}O$) in GC-1, GC-3, GC-4, ooids Halimeda, Penicillus, Rhiphocephalus and sedimentary aragonite needles.*

Core no.	Depth interval (cm)	Aragonite (wt%)	δ^{13}C (V-PDB)	δ^{18}O (V-PDB)
GC-1	115–120	79	2.6	−.5
	165–170	81	2.7	−0.2
	245–250	77	2.7	−0.1
	305–310	76	2.7	−0.3
	355–360	70	2.9	−0.1
GC-2	40–41	97	3	−0.5
	140–142	93	2.9	−0.4
	198–200	94	2.8	−0.4
	280–285	94	2.8	−0.4
	340–345	89	2.7	−0.3
	400–405	92	2.8	−0.4
	460–465	91	2.4	−0.5
	520–525	92	2.6	−0.4
GC-5	66–67	55	0.1	−0.9
	164–166	>95	3.8	1
	220–225	>95	4	1
	280–285	>95	4.4	1.4
	340–345	>95	4.3	1.3
	400–405	>95	4.3	1.3
	460–465	>95	4.4	1.3
	520–525	>95	4	0.5
GC-4	72–73	56	1	−0.7
	130–132	69	1.9	−0.2
	200–205	>95	3.8	0.1
	230–235	>95	4.1	1.1
	260–265	>95	3.8	0
	300–305	>95	3.8	0.4
	340–345	>95	4	0.4
	380–385	>95	3.8	0.8
	420–425	>95	3.8	0.8
Ooids from the platform		> 95	4.81	1.73
		>95	4.37	0.92
		>95	4.3	0.69
		>95	4.07	0.5
		>95	4.46	1.09
		>95	4.34	0.89
		>95	4.59	1.09
		>95	3.97	1.51
Halimeda#		–	4.2	−0.6
		–	2	−1.3
		–	3.8	−2.7
		–	4.2	−3.1
		–	5.5	−2.8
Penicillus#		–	2.2	−0.4
Rhiphocephalus#		–	4.4	−1.4
		–	4.4	−0.9

Table 2. *(Continued)*

Core no.	Depth interval (cm)	Aragonite (wt%)	δ^{13}C (V-PDB)	δ^{18}O (V-PDB)
Sedimentary aragonite needles#		–	4.6	0.5
		–	4.9	0.5
		–	4.2	0.2
		–	3.8	0.3
		–	3.2	−0.1
		–	2.8	−0.5
		–	2.8	−0.1
		–	3.1	−0.2
		–	3.3	0.2

#: data from Lowenstam and Epstein (1957).

muds varied from 16.1 to 14.0 ka, 12.8 to 11.9 ka and, 14.1 to 13.0 ka in GC-3, GC-4 and GC-5, respectively (figure 3; table 1).

4. Discussion

4.1 *Origin of lime muds*

The aragonite content of the lime muds (unit 2) varied from 73–80 wt% in GC-1, >90% in GC-2 and >95% in GC-3–GC-5. The lime muds therefore, are referred here as aragonite muds or aragonite-dominated lime mud.

4.1.1 *Shelf cores*

The origin of lime muds may be discussed based on their Sr content and stable isotopes. (a) The Sr values of the muds (0.29% in GC-1, 0.55% in GC-2), however, do not support inorganic origin of aragonite, because the values are much lower than the inorganic aragonite muds from the Bahamas (0.72–1.06%) or in coastal lagoons of the Abu Dhabi (0.94%) (see Bathurst 1971). The Sr values of lime muds in GC-1 and GC-2 are even lower than those in high-Sr skeletals (0.63–0.85% Sr). One may argue that low Sr content of lime muds might have been due to the dilution of other carbonate minerals and terrigenous sediments, or Sr loss during diagenesis. (b) The distinct and much depleted isotopic values of lime muds (figure 5b–c) may indicate their formation either in less saline conditions rather than in open shelf, or that the lime muds were subaerially exposed and thus altered after their formation on the shelf.

Core GC-1 is located off the Gulf of Kachchh (figure 1) which has a maximum water depth of 40 m with 5–6 m high tides. At present, lime muds do not form either in the Gulf or in the tidal flats of the Gulf of Kachchh. The older ages of the muds in core GC-1 do not agree with their formation during shallow sea level conditions of the shelf (e.g., figure 2 shows the 15 ka aged lime muds in core GC-1; the sea level was at −100 m at ∼15 ka (Fairbanks 1989), whereas GC-1 was collected at 56 m depth). Therefore, it is likely that the water in the Gulf may have been conducive for the growth of aragonite-producing plants at ∼15 ka. Subsequently, these muds were reworked, admixed with clastic sediments and exported onto the shelf. Blunt aragonite needles (figure 4a) and their association with abundant terrigenous clays (45–50%) suggest that the muds are reworked. As the transport of terrigenous sediments by river outflows may have led to a periodic bath of mud in less saline waters, the depleted isotopic values of lime muds may also arise from diagenesis. Lime muds of younger ages underneath the older muds (figure 2; table 1) support the argument that these muds were reworked. Alternatively, the lime muds are entirely from the shelf, but varying admixtures of older carbonates that exposed during low sea levels and younger carbonates. The core GC-2 is located closer to the carbonate platform. Variable Sr values (0.25–0.6%) for higher aragonite content (85–90%, figure 5a) probably suggest that the aragonite muds are mixture derived from the shelf and carbonate platform.

4.1.2 *Cores at the shelf break*

The lime muds in GC-3–GC-5 showed highest carbonate (90–95%) and aragonite (>95 wt%). The Sr content of the inorganically precipitated aragonite needles (>0.85–1%) is higher than that derived from disintegration of high-Sr (0.63–0.85%) skeletal materials (Milliman *et al* 1993). The Sr values of the lime muds (0.58–0.77%, figure 3) would be compatible with a large proportion of aragonite needles derived from post-mortem disaggregation of the high-Sr skeletals, such as corals and other codiacean algae. A few coral fragments are

known to occur on the carbonate platform (Rao *et al* 2003). Since the mechanical production of silt and clay-sized sediment from the corals is low (<2%, Milliman 1974 and upto 20%, Gischler and Zingeler 2002), larger contribution of aragonite needles may be from codiacean algae. This argument is well supported by the reported occurrence of *Halimeda* bioherms on the carbonate platform (Rao *et al* 1994). Moreover, Rao *et al* (1994) reported rounded, smaller (<2 mm) *Halimeda* grains than the actual *Halimeda* plates (5 mm) on the platform. This implies that the original *Halimeda* plates were decomposed and the muds thus produced were exported to the shelf break. Heavily fragmented prismatic aragonite needles support high-energy conditions and disintegration from aragonite secreting skeletals. The Sr/Ca ratios estimated for the lime muds in cores GC-3 (0.022–0.024) and GC-4 (0.020–0.021) are close to that of *Halimeda* (0.024) reported by Thomson *et al* (2004) and Reitz and de Lange (2006), suggesting that the muds were disintegrated from *Halimeda*. The Sr values of lime muds thus simply point to bioclastic origin.

The aragonite blades with blunt terminations and prismatic ends, rods showing rounded ends, jointed needles (figure 4e–f) and rods emanating from the envelope of mineralized aragonite (figure 4e) are typical characteristics to suggest that they were disintegrated from the soft tissues of algae (see Loreau 1982; Macintyre and Reid 1992). The stable isotope values of aragonite muds are within the range for sedimentary aragonite needles, but much higher than that for *Halimeda* and *Penicillus* (figure 5d). Despite the fact that the sedimentary aragonite needles are of organic origin (Lowenstam and Epstein 1957), their isotopic values are slightly higher than that of aragonite algae (see figure 5d).This implies that equilibrium precipitation (in isotopic composition) of needle muds occurs in algal muds undergoing decomposition.

Macintyre and Reid (1995) have shown that aragonite needles constitute only 25–40% of many of the codiacean algae. Reid and Macintyre (1998) further reported alteration in all types of skeletal grains accompanied by mineralogical changes from Mg-calcite to aragonite or *vice-versa*. They found that cryptocrystaline grains of aragonite are the fundamental source of lime muds. The lime muds studied here contained abundant aragonite with traces of (low-magnesium) calcite. There were no cryptocrystalline nannograins or minimicrites observed under SEM. This suggests that the alteration of aragonite to Mg-calcite is insignificant in the lime muds investigated here.

The aragonite needles were aggregated into spheroid and ovoid-type particles (figure 4). Such needle aggregates were also reported in the Mediterranean sapropels and suggested that these are the end products of natural disintegration of *Halimeda* (Reitz and de Lange 2006). The same explanation may be valid for the aggregates reported here. Since indurated aragonite muds were known to occur from the platform, the alternative explanation could be that the partly indurated lime muds deposited on the shelf may have been reworked by bottom currents resulting in its breakdown and formation of subrounded-to-rounded aggregates of aragonite needles. The lime muds of relatively older age occurring above that of younger age in different cores also support that the lime muds were biodetrital and exported from the platform.

4.2 *Controls on the sedimentation of lime muds*

The core GC-1 is located off the Gulf of Kachchh which was tectonically disturbed during the late Quaternary (Rao *et al* 2003). Since the lime muds in GC-1 were reworked from the Gulf of Kachchh, the history of the lime muds will be dealt separately.

The age of lime muds recovered in core GC-2–GC-5 ranges between 16.1 and 11.9 ka BP (see figures 2–3). As the cores could not penetrate the entire lime mud section and recovered only lime mud as old as 16.1 ka, it is difficult to pinpoint when lime mud production started on the platform. Moreover, the ages (between 14.3 and 7.6 ka BP) and depths (110–60 m) of surficial carbonates on the platform (Rao *et al* 2003) do not compare with that of the glacioeustatic sea level (Fairbanks 1989), or regional sea level data reported by several researchers for the Indian Ocean (Zinke *et al* 2003; Camoin *et al* 2004; Woodworth 2005; Woodroffe 2005). Younger aged carbonates at deeper depths and *vice versa* were reported on the platform (Rao *et al* 2003). It is therefore difficult to bring out the relationship between bathymetry and relative position of sea level and sites of carbonate production on the platform. Although the platform on the NW margin of India (17°–21°N; 70°–72°E) and carbonate ramp on the NW Australia (17°–18°S; 115°E) are located in different hemispheres, they exhibit similar characteristics. The period of lime mud production on the former (16.1–1.9 ka) coincides well with that of lime muds and ooids production (15–12 ka) on the latter (Dix *et al* 2005; James *et al* 2005); this suggest similar environmental conditions (low stands of sea level and tropical climate) for carbonate mud production. After 11.9 ka BP, the lime mud sediment deposition gradually changed to terrigenous–dominated sediments (figures 2 and 3). Van Campo (1986) and Sirocko *et al* (2000) reported that the SW monsoon was reactivated after the LGM with its maxima intensity after the Younger Dryas event at ∼11.5 ka.

Rapid rise in sea level was also reported at ∼12 ka BP. The climate change that induced a flood of siliciclastics, and rapid rise in sea level probably terminated suitable conditions for carbonate mud production. James *et al* (2005) and Dix *et al* (2005) proposed changing oceanography and rapid rise in sea level for the termination of carbonate muds off the NW Australia. It thus appears that the production and termination of carbonate muds during the late Quaternary was a regional event in the Indian Ocean and associated with low stands of sea level.

5. Conclusions

Lime muds occurred abundantly in the lower sections of the five sediment cores collected off the northwest India. The lime muds were admixed with 25–40% terrigenous material on the shelf but <5% terrigenous material at the shelf break. Lime muds were dominated by aragonite. The Sr content, SEM and isotope studies and radiocarbon ages of lime mud indicate that the lime muds are biodetrital, formed at low stands of sea level with a potential freshwater contribution for those on the shelf and purely marine contribution for those at the shelf break. The change from lime mud-dominated to terrigenous-dominated sediments after 12 ka may be due to climate change and rapid rise in sea level during the early Holocene.

Acknowledgements

The authors thank the Director, National Institute of Oceanography for facilities and encouragement. Dr. Meloth Thamban helped the senior author in subsampling the sediment cores onboard. AAK thanks CSIR for awarding research fellowship. Mr. David Wheeler, Australia helped the authors with stable isotope analyses. This is NIO contribution no. 5125.

References

Adjas A, Masse J P and Montaggioni L F 1990 Fine-grained carbonates in nearly closed reef environment: Mataiva and Takapoto atolls, Central Pacific Ocean; *Sedim. Geol.* **67** 115–132.

Basu D N, Banerjee A and Tamhane D M 1980 Source areas and migration trends of oil and gas in Bombay offshore Basin, India; *Am. Assoc. Petrol. Geol. Bull.* **64** 209–220.

Bathurst R G C 1971 *Carbonate Sediments and their diagenesis*; Elsevier, Amsterdam.

Boardman M R and Carney C 1991 Origin and accumulation of lime mud in ooid tidal channels, Bahamas; *J. Sedim. Petrol.* **61** 661–680.

Broecker W S and Takahashi T 1966 Calcium carbonate precipitation on the Bahama Bank; *J. Geophys. Res.* **71** 1575–1602.

Camoin G F, Montaggiono L F and Braithwaite C J R 2004 Late glacial to post-glacial sea levels in the western India Ocean; *Mar. Geol.* **206** 119–146.

Chivas A R, De Deckker P, Wang S X and Cali J A 2002 Oxygen isotope systematics of the nektic ostracod *Australocypris robusta*, In: The Ostracoda: Applications in Quaternary Research; *Am. Geophys. Union, Geophys. Monograph* **131** 301–313.

Cloud P E Jr 1962 Environment of calcium carbonate deposition west of Andros Island, Bahamas; USGS Professional Paper 350, 138p.

De Groot K 1965 Inorganic precipitation of calcium carbonate from sea water; *Nature* **207** 404–405.

Dix G R 2001 Origin of Sr-rich magnesiian calcite mud in a Holocene pond basin (Lee Stocking Island, Bahamas); *J. Sedim. Res.* **71** 167–175.

Dix G R, James N P, Kyser T K, Bone Y and Collins L B 2005 Genesis and dispersal of carbonate mud relative to Late Quaternary sea-level change along a distally-steepened carbonate ramp (Northwestern shelf, western Australia); *J. Sedim. Res.* **75** 665–678.

Dutta K, Bhushan R and Somayajulu B L K 2001 ΔR correction values for the northern Indian Ocean; *Radiocarbon* **43** 483–488.

Fairbanks R G 1989 A 17,000 year glacio-eustatic sea-level record: Influence of glacial melting rates on Younger Dryas event and deep ocean circulation; *Nature* **342** 637–642.

Gischler E and Lomando A 1999 Recent sedimentary facies of isolated carbonate platforms, Belize-Yucatan system, Central America; *J. Sedim. Res.* **69** 747–763.

Gischler E and Zingeler D 2002 The origin of carbonate mud in isolated carbonate platforms of Belize, Central America; *Int. J. Earth Sci.* **91** 1054–1070.

Ginsburg R N 1956 Environmental relationships of grain size and constituent particles in some south Florida carbonate sediments; *Am. Assoc. Petrol. Geol. Bull.* **40** 2384–2427.

James N P, Collins L B, Bone Y and Hallock P 1999 Subtropical carbonates in a temperate realem: Modern sediments on the southwest Australian shelf; *J. Sedim. Res.* **69** 1297–1321.

James N P, Bone Y, Collins L B and Kyser T K 2001 Surficial sediment of the Great Australian Bight: Facies dynamics and oceanography on a vast cool-water carbonate shelf; *J. Sedim. Res.* **71** 549–567.

James N P, Bone Y, Kyser T K, Dix GR and Collins L B 2004 The importance of changing oceanography in controlling late Quaternary carbonate sedimentation on a high-energy, tropical oceanic ramp, Northwestern Australia; *Sedimentology* **51** 1179–1205.

James N P, Bone Y and Kyser T K 2005 Where has all the aragonite gone? Mineralogy of Holocene neretic cool water carbonates, southern Australia; *J. Sedim. Res.* **75** 454–463.

Loreau J-P 1982 Sédiments aragonitiques et leur genèse; *Mémoires du Museum National d'Histoire Naturelle* **47** 312p.

Lowenstam H A and Epstein S 1957 On the origin of sedimentary aragonite needles of the Great Bahama Bank; *J. Geol.* **65** 364–375.

Matthews R K 1966 Genesis of recent lime mud in Southern British Honduras; *J. Sedim. Petrol.* **36** 428–454.

Macintyre I G and Reid R P 1992 Comment on the origin of Bahamian aragonitic mud: A picture is worth a thousand words; *J. Sedim. Petrol.* **67** 1095–1097.

Macintyre I G and Reid R P 1995 Crystal alteration in a living calcareous Alga (Halimeda): Implications for studies in skeletal diagenesis; *J. Sedim. Res.* **A65** 143–153.

Marshall J F and Davies P J 1988 *Halimeda* bioherms of the northern Great Barrier Reef; *Coral Reefs* **6** 139–148.

Milliman J D 1974 Marine Carbonates; Springer-Verlag, Heidelberg.

Milliman J D, Freile D, Steinen R P and Wilber R J 1993 Great Bahama Bank aragonitic muds: mostly inorganically precipitated, mostly exported; *J. Sedim. Petrol.* **63** 589–595.

Mitterer R M 1972 Biogeochemistry of aragonite mud and ooids; *Geochim Cosmochim Acta* **36** 1407–1422.

Morse J W and Mackenzie F T 1990 Geochemistry of sedimentary carbonates; In: *Developments in Sedimentology* (New York: Elsevier), **48** 707p.

Morse J W, Millero F J, Thurmond V, Brown E and Ostlund H G 1984 Carbonate chemistry of Grand Bahama Bank waters: After 18 years another look; *J. Geophys. Res.* **89** 3604–3614.

Nair R R 1971 Beach rock and associated carbonate sediments on the Fifty Fathom Flat, a submarine terrace on the outer continental shelf off Bombay; *Proc. Indian Acad. Sci.* **73B** 148–154.

Nair R R, Hashimi N H and Guptha M V S 1979 Holocene limestones of part of the western continental shelf of India; *J. Geol. Soc. India* **20** 17–23.

Neumann A C and Land L S 1975 Lime mud deposition and calcareous algae in the Bight of Abaco, Bahamas: A budget; *J. Sedim. Petrol.* **45** 763–786.

Rao V P and Wagle B G 1997 Geomorphology of the western continental shelf and slope of India: A review; *Curr. Sci.* **73** 330–350.

Rao V P, Veerayya M, Nair R R, Dupeuble P A and Lamboy M 1994 Late Quaternary *Halimeda* bioherms and aragonitic faecal pellet-dominated sediments on the carbonate platform of the western continental shelf of India; *Mar. Geol.* **121** 293–315.

Rao V P, Rajagopalan G, Vora K H and Almeida F 2003 Late Quaternary sea level and environmental changes from relic carbonate deposits of the western margin of India; *Proc. Indian Acad. Sci. (Earth Planet. Sci.)* **112** 1–25.

Reid R P and Macintyre I G 1998 Carbonate recrystallization in shallow marine environments: A widespread diagenetic process forming micritized grains; *J. Sedim. Petrol.* **68** 928–946.

Reid R P, Macintyre I G and Post J E 1992 Micritized skeletal grains in northern Belize lagoon: A major source of Mg-calcite mud; *J. Sedim. Petrol.* **62** 145–156.

Reitz A and De Lange G J 2006 Abundant Sr-rich aragonite in eastern Mediterranean Sapropel S1: Diagenetic *vs.* detrital/biogenic origin; *Palaeogeol. Palaeoclimat. Palaeoecol.* **235** 135–148.

Robbins L L and Blackwelder P L 1992 Origin of whitings: A biologically induced non-skeletal phenomenon; *Geology* **20** 464–467.

Roth S and Reijmer J J G 2004 Holocene Atlantic climate variations deduced from carbonate peri-platform sediments (leeward margin, Great Bahama Bank); *Paleoceano.* **19** PA1003, doi: 10.1029/2003PA000885.

Roth S and Reijmer J J G 2005 Holocene millennial to centennial carbonate cyclicity recorded in slope sediments of the Great Bahama Bank and its climatic implications; *Sedimentology* **52** 161–181.

Shinn E A, Steinen R P, Lidz B H and Swart P K 1989 Whitings: A sedimentological dilemma; *J. Sedim. Petrol.* **59** 147–161.

Sirocko F, Schonberg D G and Deve Y C 2000 Processes controlling trace element geochemistry of Arabian Sea sediments during the last 25,000 years; *Global Planet Change* **26** 217–303.

Steinen R P, Swart P K, Shinn E A and Lidz B H 1988 Bahamian lime mud: The algae didn't do it (Abstract); *Geol. Soc. Am.* Abstract with Program, A209.

Stockman K W, Ginsburg R N and Shinn E A 1967 The production of lime mud by algae in south Florida; *J. Sedim. Petrol.* **37** 633–648.

Stuiver M, Reimer PJ, Bard E, Beck J W, Burr G S, Hughen K A, Kromer B, Mc Cormac F G, Van Der Plicht J and Spurk M 1998 INTCAL 98 radiocarbon age calibration, 24,000-0 cal BP; *Radiocarbon* **40** 1041–1083.

Thomson J, Crudeli D, De Lange C P, Erba E and Corselle C 2004 *Florisphaera Profunda* and the origin and diagenesis of carbonate phases in eastern Mediterranean sapropel units; *Paleoceano.* **9** PA 3003 1–19.

Van Campo E 1986 Monsoon fluctuations in two 20,000 year B.P. oxygen isotope/pollen records off south west of India; *Quat. Res.* **26** 376–388.

Vaz G, Misra V S, Biswas N R, Jayakumar P V, Krishna Rao J V, Sankar J and Faruque B M 1993 Lime mud in continental shelf edge and slope off Kachchh; *Indian J. Mar. Sci.* **22** 209–215.

Wells A J and Illing L V 1964 Present day precipitation of calcium carbonate in the Persian Gulf. In: *Deltaic and shallow marine deposits* (Amsterdam: Elsevier), pp. 429–435.

Woodroffe C D 2005 Late Quaternary sea level high stands in the central and eastern Indian Ocean A review; *Global Planet. Change* **49** 121–138.

Woodworth P L 2005 Have there been large recent sea level changes in the Maldive Islands? *Global Planet. Change* **49** 1–18.

Yates K K and Robbins L A 1999 Radioisotope tracer studies of inorganic carbon and Ca in microbially derived $CaCO_3$; *Geochim Cosmochim Acta* **63** 129–136.

Zinke J, Reijmer J J G, Thomassin B A, Dullo W-C, Grootes P M and Erlenkeuser H 2003 Postglacial flooding history of Mayotte lagoon (Comoro archipelago, southwest Indian Ocean); *Mar. Geol.* **194** 181–196.

MS received 8 January 2011; revised 14 January 2012; accepted 16 January 2012